

Multispecies reaction diffusion models and the Turing instability revisited

D. Fanelli^{1,3}, C. Cianci^{2,3}, F. Di Patti¹

1. *Dipartimento di Energetica, Università degli Studi di Firenze, via S. Marta 3, 50139 Florence, Italy*

2. *Dipartimento di Sistemi e Informatica, Università degli Studi di Firenze, via S. Marta 3, 50139 Florence, Italy*

3. *INFN, Sezione di Firenze, via G. Sansone 1, 50019 Sesto Fiorentino, Florence, Italy*

(Dated: January 27, 2019)

The Turing instability paradigm is revisited in the context of a multispecies diffusion scheme derived from a self-consistent microscopic formulation. The analysis is developed with reference to the case of two species. These latter share the same spatial reservoir and experience a degree of mutual interference due to the competition for the available resources. Turing instability can set in for all ratios of the main diffusivities, also when the activator diffuses faster than the inhibitor. This conclusion, at odd with the conventional vision, is here exemplified for the Brusselator model and ultimately stems from having assumed a generalized model of multispecies diffusion, fully anchored to first principles, which also holds under crowded conditions.

PACS numbers: 87.23.Cc, 02.50.-r, 05.10.Ln

Turing instability constitutes a universal paradigm for the spontaneous generation of spatially organized patterns [1, 2]. It formally applies to a wide category of phenomena, which can be modeled via reaction diffusion schemes [3, 4]. These are mathematical models that describe the coupled evolution of spatially distributed species, as driven by microscopic reactions and freely diffusing in the embedding medium. Diffusion can potentially seed the instability by perturbing the mean-field homogeneous state, through an activator-inhibitor mechanism, and so resulting in the emergence of patched, spatially inhomogeneous, density distribution. The most astonishing examples are encountered in the context of morphogenesis, the branch of embryology devoted to investigating the development of patterns and forms in biology. The realm of application of the Turing ideas encompasses however different fields, ranging from chemistry [5] to biology [3, 6–10], passing through physics [11], where large communities of homologous elements evolve and mutually interact.

Beyond the qualitative agreement, one difficulty in establishing a quantitative link between theory and empirical observations has to do with the strict conditions for which the organized Turing patterns are predicted to occur. In particular, according to the classical viewpoint, the diffusion coefficient of the inhibitor species has to be larger than that of the activator, for the patterns to eventually develop. This is a strict mathematical constraint which however clashes with experiments: spatially extended systems made of interacting species sharing similar diffusivities can indeed display patched patterns. This observation still calls for a sound interpretative scenario, beyond the classical Turing mechanisms [1].

One viable strategy to possibly reconcile theory and observations has been explored in [12] and [13]. In these studies, the authors considered the spontaneous emergence of persistent spatial patterns as mediated by the demographic endogenous noise, stemming from the intimate discreteness of the scrutinized system. The intrinsic noise translates into a systematic enlargement of the parameter region yielding to the Turing order, when compared to the corresponding domain predicted within the deterministic linear stability analysis. It is however unclear at present whether experimentally recorded patterns bear the imprint of the stochasticity, a possibility that deserves to be further challenged in the future.

Alternatively, and to bridge the gap with the experiments, the Turing instability concept has been applied to generalized reaction-diffusion equations. These latter account for cross diffusion terms which are hypothesized to exist on purely heuristic grounds or by invoking the phenomenological theory of linear non-equilibrium thermodynamics [14]. Diagonal and off-diagonal coefficients of the diffusion matrix are not linked to any microscopic representation of the examined dynamics and are hence treated as free parameters of the model. In [15] the authors quantify the impact of cross terms on the Turing bifurcation, showing e.g that spatial order can materialize also if the inhibitor's diffusion ability is less pronounced than the activator's one.

Starting from this setting, the aims of this paper are twofold. On the one side, we shall elaborate on a microscopic theory of multispecies diffusion, fully justified from first principles. The theory here derived is specifically targeted to the two species case study and extends beyond the formulation of [16]. On the other side, and with reference to the Brusselator model, we will show that Turing patterns can take place for any ratio of the main diffusivities. In doing so we will cast the conclusions of [15] into a descriptive framework of broad applied and fundamental interest, where the key cross diffusion ingredients are not simply guessed a priori but rigorously obtained via a self-consistent derivation anchored to the microscopic world.

In the following we briefly discuss the derivation of the model, focusing on the specific case where two species are supposed to diffuse, sharing the same spatial reservoir. Consider a generic microscopic system bound to occupy

a given volume of a d -dimensional space. Assume the volume to be partitioned into a large number Ω of small hypercubic patches, each of linear size l . Each mesoscopic cell, labeled by i , is characterized by a finite carrying capacity: it can host up to N particles, namely n_i^A of type A , n_i^B of type B , and $v_i = N - n_i^A - n_i^B$ vacancies, hereafter denoted by V . In general, the species will also interact, as dictated by specific reaction terms. Let us start by solely focusing on the diffusion part, silencing any direct interaction among elementary constituents. As we shall remark, there exists an indirect degree of coupling that results from the competition for the available spatial resources. In practice, the mobility of the particles is balked if the neighboring patches have no vacancies. Particles may jump into a nearest-neighbor patch, only if there is a vacancy to be eventually filled. This mechanism translates into the following chemical equation



where i and j label nearest-neighbor patches. Here, A_i and B_i identify the particles that belong to cell i . V_i labels instead the empties that are hosted in patch i . The parameters μ^A and μ^B stand for the associated reaction rates. Similar reactions control the migration from cell j towards cell i .

In addition, and extending beyond the scheme proposed in [16], we imagine the following reactions to hold:



which in practice account for the possibility that elements A_i (resp. A_j) and B_j (resp. B_i) swap their actual positions.

The state of the system is then specified by the number of A and B particles in each patch, the number of vacancies following from a straightforward normalization condition. Introduce the vector $\mathbf{n} = (\mathbf{n}_1, \dots, \mathbf{n}_\Omega)$, where $\mathbf{n}_i = (n_i^A, n_i^B)$. The quantity $T(\mathbf{n}'|\mathbf{n})$ represents the rate of transition from state \mathbf{n} , to another state \mathbf{n}' , compatible with the former. The transition rates associated with the migration between nearest-neighbor, see Eqs. (1), take the form

$$T(n_i^{(a)} - 1, n_j^{(a)} + 1 | n_i^{(a)}, n_j^{(a)}) = \frac{\mu^{(a)}}{z\Omega} \frac{n_i^{(a)}}{N} \frac{N - n_j^A - n_j^B}{N}, \quad a = A, B, \quad (3)$$

where we have explicitated in $T(\cdot|\cdot)$ the components that are affected by the reactions. As discussed in [16], the factor $N - n_j^A - n_j^B$, reflects the natural request of a finite capacity, and will eventually yield to a macroscopic modification of the Fick's law of diffusion. Moreover, chemical equations (2) result in the following transition rates:

$$\begin{aligned} T(n_i^A - 1, n_j^A + 1, n_i^B + 1, n_j^B - 1 | n_i^A, n_j^A, n_i^B, n_j^B) &= \frac{\alpha}{z\Omega} \frac{n_i^A}{N} \frac{n_j^B}{N}, \\ T(n_i^A + 1, n_j^A - 1, n_i^B - 1, n_j^B + 1 | n_i^A, n_j^A, n_i^B, n_j^B) &= \frac{\alpha}{z\Omega} \frac{n_j^A}{N} \frac{n_i^B}{N}. \end{aligned} \quad (4)$$

The process here imagined is Markov, and the probability $P(\mathbf{n}, t)$ to observe the system in state \mathbf{n} at time t is ruled by the master equation

$$\frac{dP(\mathbf{n}, t)}{dt} = \sum_{\mathbf{n}' \neq \mathbf{n}} [T(\mathbf{n}|\mathbf{n}')P(\mathbf{n}', t) - T(\mathbf{n}'|\mathbf{n})P(\mathbf{n}, t)], \quad (5)$$

where the allowed transitions depend on the state of the system via the above relations. Starting from this microscopic, hence inherently stochastic picture, one can derive a self-consistent deterministic formulation, which exactly holds in the continuum limit. Mathematically, one needs to obtain the dynamical equations that govern the time evolution of the ensemble averages $\langle n_i^A \rangle$ and $\langle n_i^B \rangle$. To this end, multiply first the master Eq. (5) by n_i^a , with $a = A, B$, and sum over all \mathbf{n} . After an algebraic manipulation which necessitates shifting some of the sums by ± 1 , one eventually gets

$$\begin{aligned} \frac{d\langle n_i^{(a)} \rangle}{dt} &= \sum_{j \in i} \left[\langle T(n_i^{(a)} + 1, n_j^{(a)} - 1 | n_i^{(a)}, n_j^{(a)}) \rangle + \langle T(n_i^A + 1, n_j^A - 1, n_i^B - 1, n_j^B + 1 | n_i^A, n_j^A, n_i^B, n_j^B) \rangle \right. \\ &\quad \left. - \langle T(n_i^{(a)} - 1, n_j^{(a)} + 1 | n_i^{(a)}, n_j^{(a)}) \rangle - \langle T(n_i^A - 1, n_j^A + 1, n_i^B + 1, n_j^B - 1 | n_i^A, n_j^A, n_i^B, n_j^B) \rangle \right], \end{aligned} \quad (6)$$

where the notation $\sum_{j \in i}$ means that we are summing over all patches j which are nearest-neighbors of patch i . The averages in Eq. (6) are performed explicitly by recalling the expression for the transition rates as given in Eqs. (3)

and (4). Replace then the averages of products by the products of averages, an operation that proves exact in the continuum limit $N \rightarrow \infty$. By introducing the continuum concentration $(\phi_{A,B})_i = \lim_{N \rightarrow \infty} \frac{\langle n_{i,A,B} \rangle}{N}$, rescaling time by a factor of $N\Omega$ and taking the size of the patches to zero one finally gets [17]

$$\begin{aligned}\frac{\partial \phi_A}{\partial t} &= D_{11} \nabla^2 \phi_A + D_{12} [\phi_A \nabla^2 \phi_B - \phi_B \nabla^2 \phi_A], \\ \frac{\partial \phi_B}{\partial t} &= D_{22} \nabla^2 \phi_B + D_{21} [\phi_B \nabla^2 \phi_A - \phi_A \nabla^2 \phi_B],\end{aligned}\quad (7)$$

where $D_{11,22} \rightarrow l^2 \mu_{A,B}$ and $D_{12,21} \rightarrow l^2 (\mu_{A,B} - \alpha)$ [18]. The above system of partial differential equations for the concentration ϕ_A and ϕ_B is a slightly modified version of the one derived in [16], this latter being formally recovered when setting α to zero. In the generalized context here considered, the cross diffusion coefficients D_{12} and D_{21} are different, specifically smaller, than the corresponding mean diffusivities D_{11} and D_{22} . We emphasize again that the crossed, nonlinear contributions $\pm(\phi_{A,B} \nabla^2 \phi_{B,A} - \phi_{B,A} \nabla^2 \phi_{A,B})$ stem directly from the imposed finite carrying capacity and, as such, have a specific, fully justified, microscopic origin. The diffusive fluxes that drive the changes in the concentrations ϕ_A and ϕ_B can be written as:

$$\begin{aligned}\mathbf{J}_{\phi_A} &= -D_{11} \left(1 - \frac{D_{12}}{D_{11}} \phi_B\right) \nabla \phi_A - D_{12} \phi_A \nabla \phi_B \\ \mathbf{J}_{\phi_B} &= -D_{21} \phi_B \nabla \phi_A - D_{22} \left(1 - \frac{D_{21}}{D_{22}} \phi_A\right) \nabla \phi_B\end{aligned}\quad (8)$$

It is interesting to notice that relations (8) enable us to make contact with the field of linear non-equilibrium thermodynamics (LNET), a branch of statistical physics which defines the general framework for the macroscopic description of e.g. transport processes. One of the central features of LNET is the relation between the forces, which cause the state of the system to change, and the fluxes, which are the result of these changes [14]. Within the formalism of LNET the fluxes \mathbf{J}_{ϕ_A} and \mathbf{J}_{ϕ_B} that rule the diffusion of the two species ϕ_A and ϕ_B are linearly related to the forces, the gradients of the respective concentrations. The quantities that establish the formal link between forces and fluxes are the celebrated Onsager coefficients, postulated on pure heuristic grounds. Interestingly, eqs (8) provide a self-consistent derivation for the Onsager coefficients, that enters the generalized Fick's scenario here depicted.

Define $\Phi = (\phi_A, \phi_B)$ and $\mathbf{J} = (J_{\phi_A}, J_{\phi_B})$. Then Eqs. (7) can be written in the compact form:

$$\frac{\partial \Phi}{\partial t} = -\nabla \mathbf{J} = \nabla \mathbf{D}(\Phi) \nabla \Phi \quad (9)$$

where the 2×2 matrix \mathbf{D} reads:

$$\mathbf{D}(\Phi) = \begin{pmatrix} D_{11} \left(1 - \frac{D_{12}}{D_{11}} \phi_B\right) & D_{12} \phi_A \\ D_{21} \phi_B & D_{22} \left(1 - \frac{D_{21}}{D_{22}} \phi_A\right) \end{pmatrix}. \quad (10)$$

A stringent constraint from thermodynamics is that all eigenvalues of the diffusion matrix \mathbf{D} are real and positive. This in turn corresponds to requiring $\text{tr}(\mathbf{D}) > 0$ and $\det(\mathbf{D}) > 0$. A straightforward calculation yields to:

$$\begin{aligned}\text{tr}(\mathbf{D}) &= D_{11}(1 - \phi_B) + D_{22}(1 - \phi_A) + \Delta D(\phi_A + \phi_B) \\ \det(\mathbf{D}) &= D_{11}D_{22}(1 - \phi_A - \phi_B) + \Delta D(D_{11}\phi_A + D_{22}\phi_B)\end{aligned}\quad (11)$$

where $\Delta D \equiv D_{11} - D_{12} = D_{22} - D_{21}$. By definition $\Delta D > 0$. Moreover, ϕ_A and ϕ_B are both positive and smaller than one. Hence, $\text{tr}(\mathbf{D}) > 0$ and $\det(\mathbf{D}) > 0$, a result that points to the consistency of the proposed formulation.

Having derived a plausible macroscopic description for the two components diffusion process, we can now move on by allowing the involved species to interact and so consequently consider in the mathematical model the corresponding reaction terms. As an important remark, we notice that these latter can be also obtained as follows the above, rather general, approach that bridges micro and macro realms. First, one need to resolve the interactions among individual constituents, by translating into chemical equations the microscopic processes implicated. These include cooperation and competition effects, as well as the indirect interferences stemming from the finite carrying capacity that we have imposed in each mesoscopic patch. Then, one can recover the deterministic equations for the global concentrations, by operating in the continuum system size limit. In general, Eq. (12) is modified into:

$$\frac{\partial \Phi}{\partial t} = \mathbf{F}(\Phi) + \nabla \mathbf{D} \nabla \Phi \quad (12)$$

where $\mathbf{F} = (f_A(\phi_A, \phi_B), f_B(\phi_A, \phi_B))$. As we have anticipated, the interest of this generalized formulation, resides in that it allows for Turing like patterns formation in a region of the parameter space that is instead forbidden when conventional reaction–diffusion systems are considered. The novelty of the proposed formulation has to do with the presence of specific cross diffusion terms, which follow a sound physical request, and add to the classical Laplacians, signature of Fickian diffusion.

Let $\hat{\phi}_A, \hat{\phi}_B$ be the steady state solution of the homogeneous (aspatial) system, namely $f_A(\hat{\phi}_A, \hat{\phi}_B) = f_B(\hat{\phi}_A, \hat{\phi}_B) = 0$. The fixed point is linearly stable if the Jacobian matrix \mathbf{A}

$$\mathbf{A} = \begin{pmatrix} \frac{\partial f_A}{\partial \phi_A} & \frac{\partial f_A}{\partial \phi_B} \\ \frac{\partial f_B}{\partial \phi_A} & \frac{\partial f_B}{\partial \phi_B} \end{pmatrix},$$

has positive determinant and negative trace. It is worth stressing that the derivatives in matrix \mathbf{A} are evaluated at the homogeneous fixed point. Back to the complete model, a spatial perturbation superposed to the homogeneous fixed point can get unstable if specific conditions are met. Such conditions, inspired to the seminal work by Turing, are hereafter derived via a linear stability analysis. Define $\eta = \Phi - \hat{\Phi}$ and proceed with a linearization of Eq. (12) to eventually obtain:

$$\frac{\partial \eta}{\partial t} = \mathbf{A}(\hat{\Phi})\eta + \mathbf{D}(\hat{\Phi})\nabla^2 \eta$$

Going to Fourier space one gets:

$$\frac{d\tilde{\eta}}{dt} = \mathbf{A}^*(k)\tilde{\eta} \quad (13)$$

where $\mathbf{A}^*(k) = \mathbf{A}(\hat{\Phi}) - k^2 \mathbf{D}(\hat{\Phi})$. By characterizing the eigenvalues of the matrix \mathbf{A}^* , one can determine whether a perturbation to the homogeneous solution can yield to patterns formation. In particular, if one of the eigenvalues admits a positive real part for some values of k , then a spatially modulated instability develops. The growth of the perturbation as seeded by the linear instability will saturate due to the non linearities and eventually results in a characteristic pattern associated to the unstable mode k . Steady patterns of the Turing type require in addition that the imaginary part of the eigenvalues associated to the unstable mode are zero. In formulae, the Turing instability sets in if there exists a k such that $\text{tr}(\mathbf{A}^*(k)) < 0$ and $\det(\mathbf{A}^*(k)) < 0$. These latter conditions are to be imposed, jointly with the request of a stable homogeneous fixed point ($\text{tr}(\mathbf{A}) < 0$, $\det(\mathbf{A}) > 0$), to identify the parameters' values that drive the instability. Alternatively, one can obtain a set of explicit conditions following the procedure outlined below, and adapted from [13]. The eigenfunctions of the Laplacian operator are:

$$(\nabla^2 + k^2) \mathbf{W}_k(\mathbf{r}) = 0,$$

and we write the solution to Eq. (13) in the form:

$$\mathbf{x}(t, \mathbf{r}) = \sum_k e^{\lambda t} a_k \mathbf{W}_k(\mathbf{r}). \quad (14)$$

By substituting the ansatz (14) into Eq. (13) yields:

$$e^{\lambda t} [\mathbf{A} - k^2 \mathbf{D} - \lambda \mathbf{1}] \mathbf{W}_k = 0.$$

The above system admits a solution if the matrix $\mathbf{A} - k^2 \mathbf{D} - \lambda \mathbf{1}$ is singular, i.e.:

$$\det(\mathbf{A} - k^2 \mathbf{D} - \lambda \mathbf{1}) = 0. \quad (15)$$

The solutions $\lambda(k)$ of (15) can be interpreted as dispersion relations. If at least one of the two solutions displays a positive real part, the mode is unstable, and the dynamics drives the system towards a non-homogeneous configuration in response to the initial perturbation. Introduce the auxiliary quantity Γ defined as:

$$\Gamma = D_{11} \frac{\partial f_B}{\partial \phi_B} + D_{22} \frac{\partial f_A}{\partial \phi_A} - \hat{\phi}_A \left[D_{21} \frac{\partial f_A}{\partial \phi_A} + D_{12} \frac{\partial f_B}{\partial \phi_A} \right] - \hat{\phi}_B \left[D_{12} \frac{\partial f_B}{\partial \phi_B} + D_{21} \frac{\partial f_A}{\partial \phi_B} \right] \quad (16)$$

Then a straightforward calculation results in the following compact conditions for the instability to occur:

$$\Gamma > 0 \quad (17)$$

$$\Gamma^2 > 4D_{11}D_{22} \left(1 - \frac{D_{12}}{D_{11}}\phi_A - \frac{D_{21}}{D_{22}}\phi_B \right) \det(\mathbf{A}) \quad (18)$$

together with $\text{tr}(\mathbf{A}) < 0$ and $\det(\mathbf{A}) > 0$.

For demonstrative purposes we now specialize on a particular case study and trace out in the parameters' plane, the domain that corresponds to the Turing instability. Our choice is to work with the Brusselator model [19] which implies setting $f_A = -(b+d)\phi_A + a(1-\phi_A-\phi_B) + c\phi_A^2\phi_B$ and $f_B = b\phi_A - c\phi_A^2\phi_B$. Species A plays now the role of the inhibitor, while B stands for the activator. Results of the analysis are reported in left panels of Fig. 1, where the region of interest is singled out in the plan (b, c) , for different choices of ΔD . Turing patterns are predicted to occur for $D_{22}/D_{11} \leq 1$, at odd with what happens in the conventional scenario where standard Fick's diffusion is assumed to hold. The right panels report the results of direct simulations and confirm the presence of macroscopically organized patterns in a region of the parameters space that is made classically inaccessible by the aforementioned, stringent condition $D_{22} > D_{11}$. The simulations refers to the choice $D_{22}/D_{11} = 0.7$. These observations are general and similar conclusions can be drawn assuming other reactions schemes of the inhibitor/activator type, different from the Brusselator model.

Summing up, Turing patterns can develop for virtually *any* ratio of the main diffusivities in a multispecies setting. This striking effect originates from the generalized diffusion theory that is here assumed to hold and that builds on the scheme discussed in [16]. Because of the competition for the available resources, a modified (deterministic) diffusive behavior is recovered: cross diffusive terms appear which links multiple diffusing communities and which add to the standard Laplacian terms, relic of Fick's law. The fact that Turing like patterns are possible for e.g. equal diffusivities

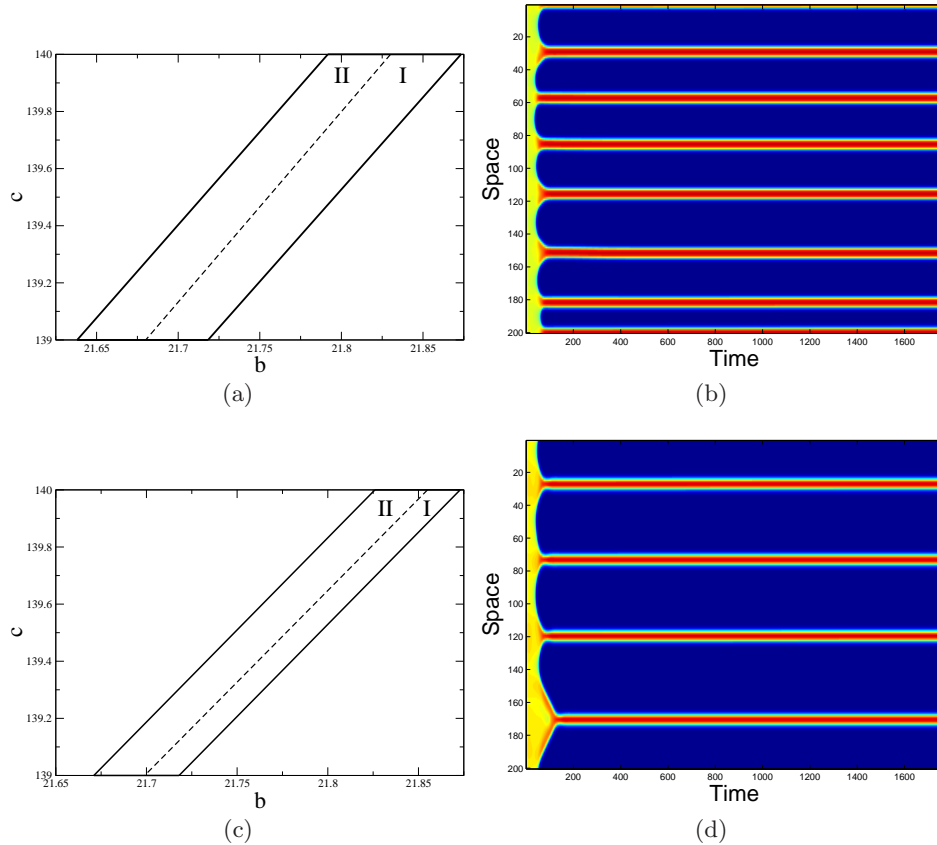


FIG. 1: Panels (a) and (c): the boundaries of the region of Turing instability are traced in the plan (b, c) , for $D_{22}/D_{11} = 1$ (panel (a)) and $D_{22}/D_{11} = 0.7$ (panel (c)). The calculated domains refer to the Brusselator model with non Fickian diffusion, as explained in the main text. The solid line, which encloses regions I and II, stands for $\Delta D = 0$, while the dashed line delimits region I, where the condition $\Delta D = 0.1$ applies. The other parameters are set as $a = 5$, $d = 3$. Panels (b) and (d): the time evolution of the concentration ϕ_A , as revealed by direct numerical simulations. In both cases, a small perturbation is superposed at $t = 0$ to the (non trivial) stable homogeneous fixed point of the Brusselator, namely $\hat{\phi}_A = (a + \sqrt{a^2 - 4ab(a+d)/c})/2/(a+d)$, $\hat{\phi}_B = b/c/\hat{\phi}_A$. Here, $D_{11} = 0.7$, $D_{22} = 1$, $b = 21.71$, $c = 139$, $a = 5$, $d = 3$. The upper right figure, panel (b), refers to $\Delta D = 0$, the lower right, panel (d), to $\Delta D = 0.1$. In the simulations we have assumed a symmetric box $[-L, L]$, with $L = 10$. The box is discretized in 200, uniformly spaced, mesh points. The simulations are run by employing an explicit Euler scheme with time step equal to 0.0001. The density in each cell of the mesh is displayed in the vertical axis, while the horizontal axis refers to the number of iterations.

of the species involved [20], as follows a sound dynamical mechanism, constitutes an intriguing observation that hold promise to eventually reconcile theory and experimental evidences. The investigated setting applies in particular to multispecies systems that evolve in a crowded environment, as it happens for instance inside the cells where different families of proteins and other biomolecular actors are populating a densely packed medium.

Acknowledgments

We wish to thank Alan McKane and Tommaso Biancalani for useful discussion. The work is supported by Ente Cassa di Risparmio di Firenze and the program PRIN2009.

-
- [1] Turing A. M. 1952, The Chemical Basis of Morphogenesis. *Philos. Trans. R. Soc. London Ser. B*, **237** 37-72 (1952).
 - [2] Buceta J., Lindenberg K. 2002, Switching-induced Turing instability. *Phys. Rev. E* **66**, 046202.
 - [3] Murray J. D., *Mathematical Biology*, Second Edition, Springer.
 - [4] Maynard Smith J. 1974, *Models in Ecology*, Cambridge University Press, Cambridge.
 - [5] Belousov B. P. 1958, A periodic reaction and its mechanism. *Collection of short papers on radiation medicine*; Zhabotinsky A. M. 1964, Periodical oxidation of malonic acid in solution (a study of the Belousov reaction kinetics). *Biofizika*, **9**, 306-311.
 - [6] Levin S. A., Segel L. A. 1976, Hypothesis for origin of planktonic patchiness. *Nature (London)* **259**, 659.
 - [7] Mimura M., Murray J. D. 1978, On a diffusive prey-predator model which exhibits patchiness. *J. Theor. Biol.* **75**, 249-262.
 - [8] Baumann M., Gross T., Feudel U. 2007, Instabilities in spatially extended predator-prey systems: Spatio-temporal patterns in the neighborhood of Turing-Hopf bifurcations. *J. Theor. Biol.* **245**, 220-229.
 - [9] Wilson W. G., Harrison S. P., Hastings A., McCann K. 1999, Exploring stable pattern formation in models of tussock moth populations. *J. Anim. Ecol.* **68**, 94-107.
 - [10] Shiferaw Y., Karma A. 2006, Turing instability mediated by voltage and calcium diffusion in paced cardiac cells. *PNAS*, **103** 15 5670-5675.
 - [11] Ammelt E., Schweng D., Purwins H.G. 1993, Spatio-temporal pattern formation in a lateral high-frequency glow discharge system *Physics Letters A* **179** Issues 4-5 348-354.
 - [12] Butler T., Goldenfeld N. 2009, Robust ecological pattern formation induced by demographic noise *Phys. Rev. E*, **80**, 030902(R).
 - [13] Biancalani T., Fanelli D., Di Patti F. 2010, Stochastic Turing patterns in the Brusselator model. *Phys. Rev. E* **81** 046215.
 - [14] de Groot S. R., Mazur P. 1984, *Non-Equilibrium Thermodynamics* (Dover, New York).
 - [15] Kumar N., Horsthemke W. 2011, Effects of cross diffusion on Turing bifurcations in two-species reaction-transport systems *Phys. Rev. E* **83** 036105.
 - [16] Fanelli D., McKane A. 2010, Diffusion in a crowded environment. *Phys. Rev. E* **82** 021113 (2010).
 - [17] Use has been made of the discrete Laplacian operator $\Delta f_i = (2/z) \sum_{j \in i} (f_j - f_i)$, which then turns into the continuum operator ∇ when sending to zero the size of the patch and scaling the rates $\mu^{A,B}$ and α appropriately.
 - [18] From the above expressions, one derives the consistency conditions $\mu_A > \alpha$ and $\mu_B > \alpha$.
 - [19] The term $a(1 - \phi_A - \phi_B)$ reflects the presence of the finite carrying capacity, as discussed in [13]. Similar conclusions hold however if the diluted limit is performed, *just* in the reaction terms, hence replacing $a(1 - \phi_A - \phi_B)$ with a .
 - [20] Notice that the authors of [13] failed to realize that accounting for cross diffusion terms of the type derived in [16] could result in an extension of the Turing mechanism to regions where $D_{22} \leq D_{11}$.